International Journal of Control and Automation
Vol.7, No.8 (2014), pp.31-42
http://dx.doi.org/10.14257/ijca.2014.7.8.04

Robust Tracking of Rhythmic Gait for a Biomimetic Robot

Chunlin Zhou[1] and K. H. Low[2]

[1]*Department of Control Science and Engineering, Zhejiang University, China 310027*
[2]*School of Mechanical & Aerospace Engineering, Nanyang Technological University, Singapore 639798*
c_zhou@zju.edu.cn, mkhlow@ntu.edu.sg

Abstract

Rhythmic movements show fundamental motion patterns in the locomotion of animals. Inspired by real animals, biomimetic robots also adopt similar locomotion pattern in order to obtain versatile mobility. For the motorized mechatronic systems in robots, trajectory tracking control of rhythmic motions is a challenge because periodical friction and other un-modeled dynamics may exist and they bring disturbance to the system. In order to enhance the tracking performance, a robust tracking controller for a biomimetic fish robot is discussed in this paper. The disturbance and the command signal will be modeled in the controller design. The controller can yield theoretically zero tracking error to a sinusoidal command input. The formulation of the controller and experimental results are presented in the paper.

Keywords: *robust tracking, rhythmic movement, gait, biomimetic robot*

1. Introduction

Rhythmic movements show fundamental motion patterns in the locomotion of animals such as the alternate swing of legs in human walking, gait transition of quadruped animals from walking to running, flapping of bird wings during flying, and oscillation of fish tail in swimming. The movement patterns of animals have inspired the design of biomimetic robots which simulate the muscles and skeletons of their animal counterparts by using mechatronics devices and adopt rhythmic gaits in the control of locomotion. The research in the control of such robots covers various aspects [1]. The gait level control of the robot implements the rhythmic trajectory on actuators of robot prototypes to ensure that the mechatronics system of biomimetic limbs can track and follow the gait control signals accurately.

For biomimetic robots where complex gait trajectories are required, rhythmic movement is directly created by motors, *i.e.*, the motor rotates bi-directionally, instead of well-designed motion transmission mechanisms such as slider-crank or a crank-rocker mechanism[2]. The purpose of control is to ensure that the movement of a mechanical manipulator can exactly track the control command signal. This is a critical requirement if there is non-decaying disturbance in the control system, for example, the alternate friction [3]. Such disturbance commonly exists in circumstances that a manipulator moves back and forth [3, 4]. Normally, PID controllers can bring satisfying tracking performance when the friction is a constant or proportional to the movement speed [5-7]. Due to the un-modeled hydrodynamics and the uncertainties among parameters of mathematical model of fish robot, it is a challenge for the motorized robot system to track the periodical gait control signals in water environment. A robust motion control system is necessary to track the gait signal and reject disturbance [8, 9].

ISSN: 2005-4297 IJCA

In this paper, a biomimetic fish robot propelled by a 2 degree-of-freedom (DoF) caudal fin will be taken as an example for the study (see Figure 1). Fish of this form obtains thrust through the oscillation of its caudal fin controlled by sinusoidal gait signals [10]. The rhythmic oscillation of the caudal fin results in continuously periodical reactive force from water, which brings strong disturbance to the control system [1]. This motor-level control problem will be the major issue of the present paper. Firstly, motion control model of the robot is discussed in Section 2. As an improvement of PD controller, the robust tracking controller, is formulated in Section 3. The performance of the PD controller and the robust tracking controller is compared and tested in experiments, which is shown in Section 4.

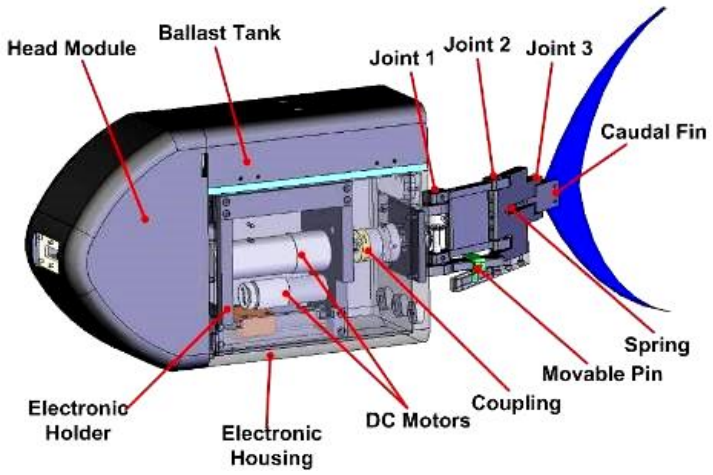

(a)

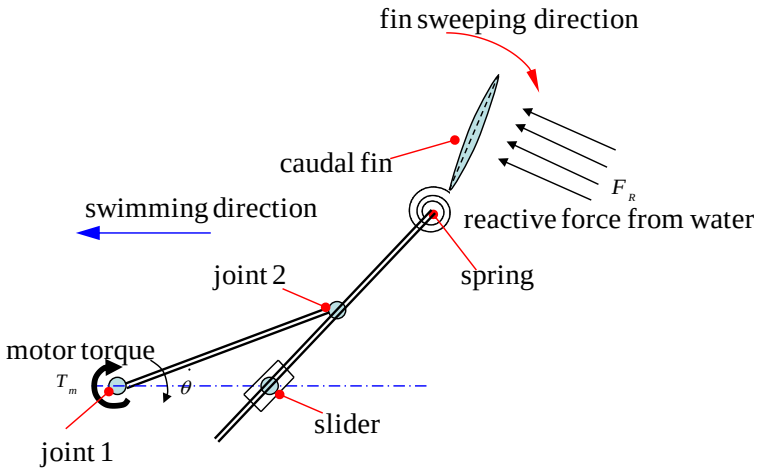

(b)

Figure 1. (a) CAD Model of a Fish Robot and (b) Schematic of Tail Linkages and the Water Reactive Force. Figures are Adapted from [11]

2. The Motion Control Model

From mechanical viewpoints, it is feasible to model vertebras of slender fish body or bones of its flexible fins as rigid linkages [12-15]. The objective of modeling swimming gait is to

find the time-dependent control signal of each actuator that drives the linkage [16, 17]. In order to maintain the coordination of multiple gaits, those gait generators can be derived from predefined motion reference system, *i.e.*, the body motion function suggested by Lighthill [13, 18]. The swimming gaits (control commands for each articulated linkages) can then be obtained by decomposing the body motion function and be modeled by a sine function during the steady swimming:

$$\theta(t) = A\sin(2\pi f t + \varphi) \tag{1}$$

where $\theta(t)$ is the gait control signal, A is the tail oscillation amplitude, f is the oscillation frequency, and φ is the phase angle between linkages. Note that A and φ are determined by the body motion function that the linkages plan to fit.

Well-selected values of the two parameters ensures the coordination of swimming motion [12, 19]. As the tail oscillates in water, the caudal fin pushes water aside and causes the distortion of water, which results in the reactive force. The force is related to the geometry of fin, the oscillation speed and the feature of fluid, as shown in Figure 1b. The water reactive force can be treated as a damping in the controller design for the tail fin [20]. The damping coefficient b is related to the geometry of caudal, the oscillation speed, the feature of fluid, and the attack angle of caudal fin to water flow. Its value can be obtained through experiments and the range is within 0.7514 - 1.12 mN·s/rad. The dynamics of the motor-linkage caudal mechanism can be given as follows [21]:

$$T_m = K_m I = (J\ddot{\theta} + b\dot{\theta}) / G \tag{2}$$

$$V_{in} - K_e \frac{\dot{\theta}}{G} = L_m \frac{dI}{dt} + IR_m \tag{3}$$

where T_m is the output torque of the motor, I is the electric current through the armature, J is the equivalent moment of inertia of the tail mechanism, and K_e is the back electromotive force coefficient. Other parameters are listed in Table 1.

Table 1. Parameters of Motion Control Model at Nominal Supply Voltage

Nominal Voltage V_{in} (V)	15
Torque constant K_m (mN·m/A)	14.3
Terminal Resistance R_m (ohm)	0.902
Terminal inductance L_m (mH)	0.0882
Tail Inertia J (gcm^2)	87.3
Nominal Gear Ratio G	180/π/103
Mechanical time constant τ (ms)	8.2

For the current mechanical system, the response delay of motor caused by the inductance of armature is much insignificant compared with the one caused by the inertia of mechanical components. Therefore the influence of the inductance can be neglected. Base on this assumption, by applying Laplace transformation to Eqs. (2) and (3), the open loop transfer function can be given by

$$\frac{\theta(s)}{\theta_d(s)} \approx \frac{GK_m}{s(JRs + bR + K_m K_e)} = \frac{K_o}{s(\tau s + 1)} \tag{4}$$

where K_o is the open loop gain, τ is the mechanical time constant, s is the Laplace operator and they are defined by:

$$\tau = \frac{RJ}{bR + K_e K_m}, \quad K_o = \frac{GK_m}{bR + K_e K_m}, \quad K_e = K_m$$

3. Design of Gait Tracking Controllers

Low level controllers are necessary to ensure the actuator accurately track the rhythmic command signal. In experiments, it has been found that once the gait signals are changed (the amplitude and/or frequency are changed), the parameters of the controller have to be redesigned if a PID controller is adopted. Otherwise, the tracking performance will be deteriorated. A robust tracking controller is developed to address this problem. The derivation of controllers is discussed in this section.

3.1. Limitation of PID Controller

The closed-loop tracking control with a fore filter is designed and described by the block diagram in Figure 2. A PD controller is adopted for the test. Integral term is absent because the control plant already contains an integrator. The fore filter is employed to eliminate the negative effect of the zero in the controller. When the controller is applied good tracking performance is only exhibited for gait signals with certain parameters. Figure 3 shows the simulation results of the tracking to different gait control inputs. Three typical cases for the control system are illustrated. The controller is designed under parameters of Case 1 and satisfied tracking performance can be observed. In Cases 2 and 3 where the amplitude and frequency are changed respectively, the tracking performance becomes worse, which indicates weak robustness of the system.

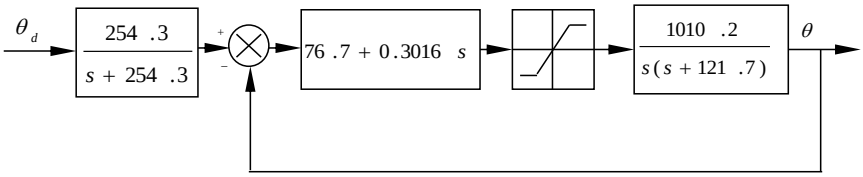

Figure 2. Closed-loop Gait Tracking Control with PD Controller and a Fore Filter

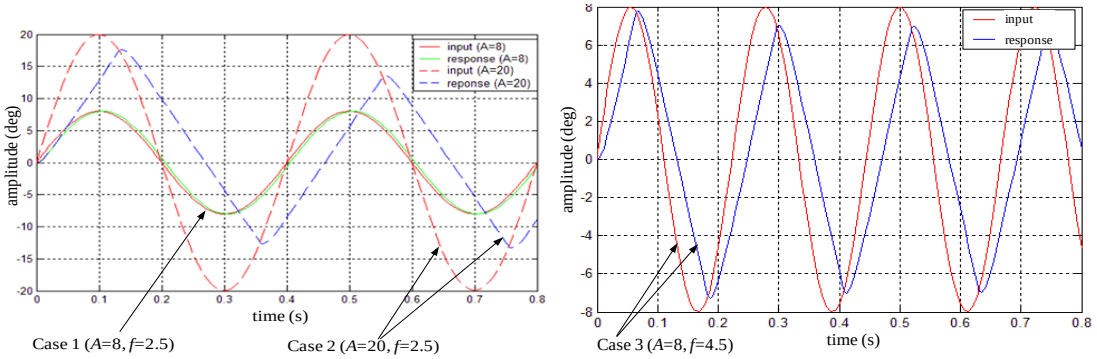

Figure 3. Tracking Performances with PD Controller for Different Gait Inputs: Response by Changing Input Amplitude (Case 2) and Influence from Change of Frequency (Case 3)

In the design of PD controller, the external reactive force is treated as linear damping to the control system. This assumption is only an approximation to the actual circumstance. The force is proportional to the square of the sweeping velocity and the damping coefficient varies periodically along with the periodical gait control input. If the input signal changes or the evaluation of damping coefficient is not accurate, the controller cannot provide high performance regulation. One way to solve this problem is to design PD controller for all input cases. However, because there are numerous combinations of input frequency and amplitude in practical application, it can hardly to develop a dynamic programmed PD controller.

3.2. Design of a Robust Gait Controller

The approach based on error space analysis and introduced in [22] will be employed to design the robust tracking system. In the state space model, the external disturbance is included. According to Eq. (4), the state space model of the tail system can be given by

$$\dot{\Theta} = \begin{bmatrix} \dot{\theta} \\ \ddot{\theta} \\ \theta \end{bmatrix} = \begin{bmatrix} 0 & 1 \\ 0 & -1/\tau \end{bmatrix} \cdot \begin{bmatrix} \theta \\ \dot{\theta} \end{bmatrix} + \begin{bmatrix} 0 \\ K_o \end{bmatrix} u + \mathbf{B}' T_R = \mathbf{A}\Theta + \mathbf{B}u + \mathbf{B}' T_R \tag{5}$$

$$y = \begin{bmatrix} 1 & 0 \end{bmatrix} \begin{bmatrix} \theta \\ \dot{\theta} \end{bmatrix} = \mathbf{C}\Theta \tag{6}$$

where $\mathbf{\Theta}$ is the system state vector, $\mathbf{A}$ is the state matrix, $\mathbf{B}$ is the input matrix, u is system input, $\mathbf{B'}$ is the disturbance matrix, y is the system output, $\mathbf{C}$ is the output matrix, and T_R is the external disturbance. Here, the disturbance is combined into control system as part of the system and the gait control problem can be solved in an error space. In this case, b=0. To build the error space, firstly the tracking error is defined by

$$e = \theta_d - y \quad i.e., \ \theta_d = e + y \tag{7}$$

By differentiating both sides of Eq. (7) twice, we obtain

$$\ddot{\theta}_d = \ddot{e} + \ddot{y} \tag{8}$$

From Eq. (1), we know that the reference gait control input satisfy the following differential equation:

$$\ddot{\theta}_d + \omega^2 \theta_d = 0 \tag{9}$$

where $\omega=2\pi f$. Substitute Eqs. (7) and (8) into (9), we obtain:

$$(\ddot{e} + \ddot{y}) + \omega^2 (e + y) = 0 \tag{10}$$

By rearranging Eq. (10), explicit input θ_d can be eliminated from those equations and the following relationship can be obtained:

$$\ddot{e} + \omega^2 e = -(\ddot{y} + \omega^2 y) = -\mathbf{C}(\ddot{\Theta} + \omega^2 \Theta) \tag{11}$$

For further deriving, new state γ is introduced. It is defined as

$$\boldsymbol{\gamma} = \ddot{\Theta} + \omega^2 \Theta = \begin{bmatrix} \gamma_1 \\ \gamma_2 \end{bmatrix} \tag{12}$$

With this definition, the Eq. (11) can be replaced by

$$\ddot{e} = -\mathbf{C}\boldsymbol{\gamma} - \omega^2 e = -\boldsymbol{\gamma}_1 - \omega^2 e \tag{13}$$

The state equation of γ can then be derived as

$$\dot{\gamma} = \dddot{\Theta} + \omega^2\dot{\Theta} = \mathbf{A}\boldsymbol{\gamma} + \mathbf{B}\mu + \mathbf{B}'(\ddot{T}_R + \omega^2 T_R) \tag{14}$$

where a new definition is introduced:

$$\mu = \ddot{u} + \omega^2 u \tag{15}$$

The disturbance satisfies the same differential equation as the gait control signal, which is

$$\ddot{T}_R + \omega^2 T_R = 0 \tag{16}$$

Substitute Eqs. (15) into (14) and obtain

$$\dot{\gamma} = \mathbf{A}\gamma + \mathbf{B}\mu = \begin{bmatrix} \gamma_2 \\ -\gamma_2 / \tau \end{bmatrix} + \begin{bmatrix} 0 \\ K_o \end{bmatrix}\mu \tag{17}$$

It can be noticed that in Eq. (17), the reference input signal θ_d and the disturbance T_R become implicit. Eqs. (13)-(17) describe the relationship between tracking error e and the newly introduced states. Then we can convert the problem of tracking reference gait input θ_d and rejecting the disturbance T_R in original system into a new problem. The tracking error e is the output of this new state space system. A suitable control law can be designed in the error space. And the new control law regulates this error space system in the order that the error tends to zero as time gets large. If the states of the new error space system can be defined as:

$$\varepsilon = \begin{bmatrix} e & \dot{e} & \gamma_1 & \gamma_2 \end{bmatrix}^T \tag{18}$$

The error space can then be defined by

$$\dot{\varepsilon} = \begin{bmatrix} 0 & 1 & 0 & 0 \\ -\omega^2 & 0 & -1 & 0 \\ 0 & 0 & 0 & 1 \\ 0 & 0 & 0 & -1/\tau \end{bmatrix} \cdot \begin{bmatrix} e \\ \dot{e} \\ \gamma_1 \\ \gamma_2 \end{bmatrix} + \begin{bmatrix} 0 \\ 0 \\ 0 \\ K_o \end{bmatrix}\mu \tag{19}$$

A full order state feedback controller is applied to the error space system. The control law is given by

$$\mu = -\begin{bmatrix} k_4 & k_3 & k_2 & k_1 \end{bmatrix} \cdot \begin{bmatrix} e \\ \dot{e} \\ \gamma_1 \\ \gamma_2 \end{bmatrix} \tag{20}$$

where k_i (i=1, 2, 3, 4) is the feedback gains. In this error space, in order to get desired dynamics and zero tracking error, we can obtain the values feedback gains through pole placing method. Theoretically, when the system performance is defined by the desired closed-loop poles, we can achieve a response with zero steady state error by pole placing method [22]. The feedback gains in Eq. (20) can then be computed through Ackermann's formula [22]. The expression of control law for the original gait control system in terms of the actual system state can then by derived. By combining Eqs. (17)-(20), we obtain:

$$\mu = \ddot{u} + \omega^2 u = -(k_4 e + k_3\dot{e}) - \begin{bmatrix} k_2 & k_1 \end{bmatrix} \cdot (\ddot{\Theta} + \omega^2\Theta) \tag{21}$$

Rearrange Eq. (21) and combine the like terms:

$$(u + \mathbf{K}\Theta)^{(2)} + \omega^2(u + \mathbf{K}\Theta) + (k_4 e + k_3 \dot{e}) = 0 \tag{22}$$

where $\mathbf{K} = [k_2, k_1]$. Eq. (22) defines the dynamics of the robust controller. It can be seen that that the system is made up of two parts. One part is the full order state feedback controller for the motor-linkage system and the other part is a feed forward regulator which can be given by the following transfer function between output of the controller x_1 and its input e:

$$\frac{w_1(s)}{e(s)} = -\frac{k_3 s + k_4}{s^2 + \omega^2} \tag{23}$$

where $\mathbf{W}=(w_1, w_2)^T$ is the state of the controller. By using this controller, the overall feedback control system can be described by the block diagram depicted in Figure 4.

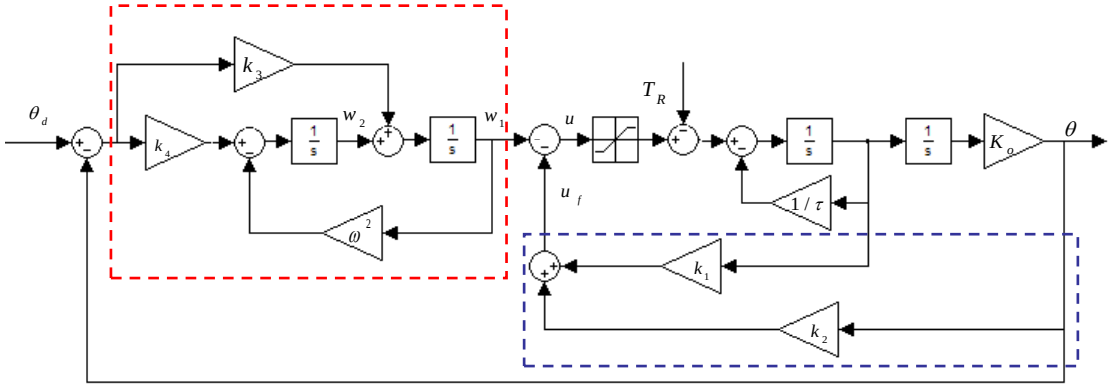

Figure 4. Block Diagram of the Closed-Loop System with a Robust Controller

It can be seen from Figure 4 that the overall control system comprises three loops. The inner loop includes the full-order feedback control loop of the plant and the feed-forward controller loop. The outer loop is an output feedback loop. The controller is actually an oscillator which shares the same frequency as the input signal and therefore as that of the disturbance. This characteristic ensures the tracking control system can accurately perform the periodical gait control input under disturbance with the same frequency. The transfer function of the full-order feedback controller is

$$\frac{u_f(s)}{\theta(s)} = k_2 + \frac{k_1}{K_o} s \tag{24}$$

According to Eq. (23) and(24), the control law of the tracking system can be given as

$$u(s) = -\frac{k_3 s + k_4}{s^2 + \omega^2} e(s) - (k_2 + \frac{k_1}{K_o} s)\theta(s) \tag{25}$$

The total open-loop system is:

$$G(s) = \frac{-k_3 K_0 (s + k_4 / k_3)}{(s^2 + \omega^2)[s^2 + (k_1 + 1/\tau)s + k_2 K]} \tag{26}$$

The transfer function of the total closed-loop system is:

$$\frac{\theta(s)}{\theta_d(s)} = \frac{-k_3K_0(s + k_4/k_3)}{s^4 + (k_1 + \frac{1}{\tau})s^3 + (k_2K_0 + \omega^2)s^2 + [\omega^2(k_1 + \frac{1}{\tau}) + k_3K_0]s + K_0(\omega^2k_2 + k_4)} \quad (27)$$

4. Experiment of Gait Tracking Control

A set of experiments has been conducted in a lab water tank to test the PD controller and the robust tracking controller. The electronic control of the robot prototype is implemented on microcontroller-based real-time hardware. Master-slave control hardware is designed to perform these functions, as depicted in Figure 5. An 8-bit micro-controller, PIC18F4520, is used as the master controller. It reads the sensor outputs and manages various tasks including sending commands, communication and task assignment. The communication with host PC is through the wireless university serial asynchronous transmission. The internal communication is based on the I^2C bus. The motion control is taken by a PIC18F2431 micro-controller. This controller runs at 40MHz, which is fast enough to perform the calculation of control algorithms. The controller generates complimentary 20KHz PWM signals to achieve a bi-directional motor control. The PWM signals are isolated from the power amplifier by an optical coupler, which enhances the stability of the electronic control system. The local controller PIC18F2431 performs the control algorithms and records the actual position data of tail fin. Then those data are transmitted through a RF transceiver to the host PC for further analysis. Upon implementation of the control algorithms, the sample rate f_s is set to 256Hz. This sample rate is fast enough to minimize the difference between the continuous and digital controller design for a DC motor driven mechanical tail system. This sample rate is chosen as the 2's integral power to make use of the shift operation in calculation, which is much faster than the normal multiplication. This technique helps to maintain the real-time property of the control system.

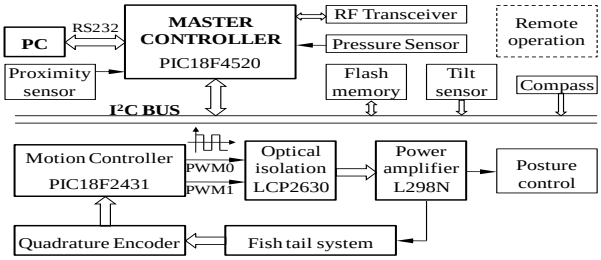

Figure 5. Control Hardware with a Master-Slave Control Hierarchy

The controller design for tail system in (25) is conducted in continuous-time domain. In order to implement the control algorithms in the digital control hardware, the Tustin transform [22] is used to convert the controller into the discrete-time domain. Figure 6 shows the responses to the gait control function with a PD controller. The testing gait is a sine signal with f=2.5Hz and A=12º. Output 1 is the experiment result with theoretical controller parameters (K_p = 76.7 and K_d =0.302). It can be seen that there is obvious discrepancy between the input and the output. Significant phase lag and tracking error appears. This discrepancy may come from the imperfect modeling of the tail system. The PD controller parameters are adjusted manually upon experiments. We increase the value of K_d to reduce the phase lag and reduce K_p to restrain large overshoots. The actual values are set to K_p = 47.5 and K_d =0.73. Accordingly, the pole and the DC gain of the fore-filter is set to 65.1. The response is shown by Output 2. We can see that the error becomes smaller but a phase lag is still remained.

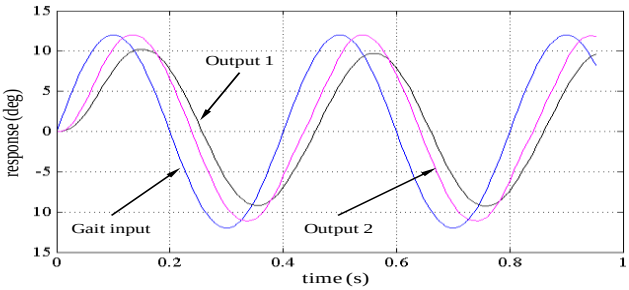

Figure 6. Experiment Results of PD Controller with Theoretical Parameters (Output 1) and Manually Adjusted Parameters (Output 2)

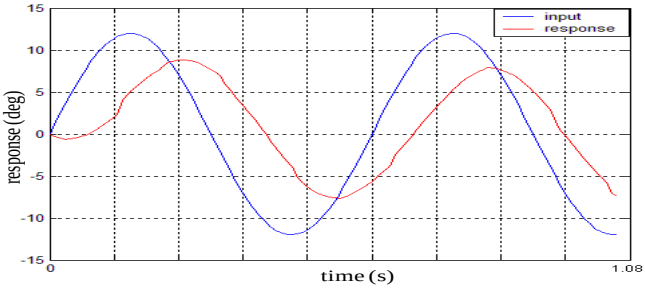

Figure 7. Experiment Results of PD Control (K_p = 47.5, K_d =0.73, f=1.75Hz, and A=12º)

In online locomotion control of fish robot, the frequency and amplitude of the swimming gait will not be constants. The PD controller has to be redesigned because in this case, the tracking control system may not be robust enough to handle different control signals. This can be illustrated by the experiment shown in Figure 7. The PD controller designed for output 2 in Figure 6 is used to tracking the gait input with f=1.75Hz and A=12º. The tracking performance becomes worse in this case as the significant difference between the input and output appears. This problem can be avoided by using the robust tracking design. By using the Tustin transform, the discrete-time version of the robust tracking control algorithms in Eq. (25) can be given by the following linear difference equation:

$$u(kT) = -\sum_{j=1}^{3} a_j u(kT - jT) + \sum_{j=0}^{3} \left[b_j e(kT - jT) + c_j y(kT - jT) \right] \tag{28}$$

where k=1, 2, 3, … and the coefficients are listed in Table 2.

Table 2. Parameters in Equation (28)

No.	j=0	j=1	j=2	j=3
a_j	0	$\frac{3\omega^2 + 4f_s^2}{\omega^2 + 4f_s^2}$	$\frac{3\omega^2 + 4f_s^2}{\omega^2 + 4f_s^2}$	1
b_j	$-\frac{k_4 + 2f_s k_3}{\omega^2 + 4f_s^2}$	$-\frac{3k_4 + 2f_s k_3}{\omega^2 + 4f_s^2}$	$\frac{2f_s k_3 - 3k_4}{\omega^2 + 4f_s^2}$	$\frac{2f_s k_3 - k_4}{\omega^2 + 4f_s^2}$
c_j	$k_2 + 2k_1 / K_o$	$k_2 - 2k_1 / K_o$	$\frac{(\omega^2 - 4f_s^2)(k_2 + 2k_1 / K_o)}{\omega^2 + 4f_s^2}$	$\frac{\omega^2 (k_2 - 2k_1 / K_o)}{\omega^2 + 4f_s^2}$

Figure 8 shows the experiment results for gait input with f=2.5Hz and A=12º. The desired input, the simulation result, the actual response from experiments and the actual error curve are shown. This gait input is selected for testing because it is the most critical control input that needs to be tracking for NAF-II (the fish cannot track inputs with higher frequency or amplitude because of the power limitation of the motor). In experiments that frequency is less than 2.5Hz, smaller tracking errors and shorter setting time are achieved. Although the ideal zero-error response is not obtained, which differs from what the theoretical analysis predicts, the tracking error is reduced significantly by this robust control after a half period of setting.

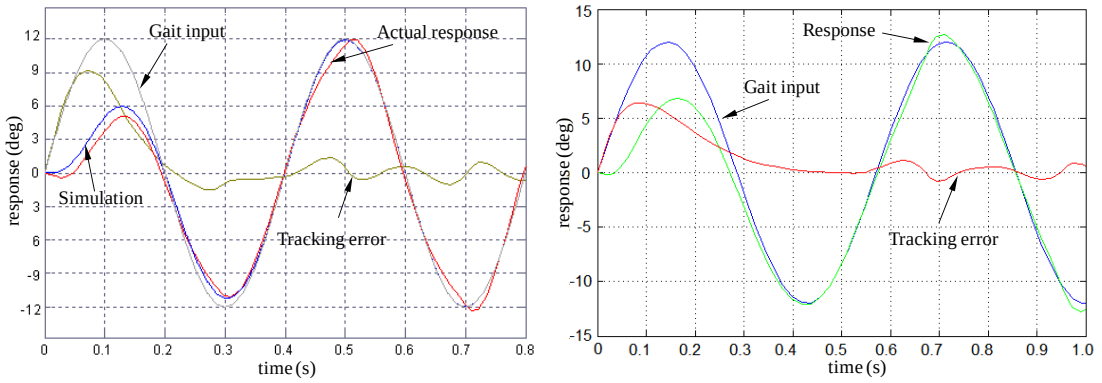

(a) (b)

Figure 8. Experimental Results of the Robust Tracking: (a) A=12º, f=2.5 Hz and (b) A=12º, f =1.75 Hz. k_1=0.0081, k_2=5.035, k_3=-81.92, k_4=150.6, and f_s=256 Hz

Because the input structure is modeled into the controller (the inner oscillator loop shown in **Figure 4**) the controller can compensate the negative effects caused by the change of input and varying external disturbance. Therefore, the robustness of the whole tail motion control system is enhanced. Additionally, an analytical solution to the robust tracking problem is given, which makes it easier to program the control algorithms dynamically. The controller parameters of the algorithm can be automatically changed by analytical equations according to the variations of the gait input. It is not necessary to try different parameters as what we do with a normal PD controller.

5. Concluding Remarks

Note that the robust tracking is in the motor control level and it does not affect the locomotion performance of a fish robot. The purpose of designing such a controller is to guarantee that an actuator can exactly follow the command signal while whether this command signal can lead to high performance of locomotion is not an issue in the present paper. Because the input structure is modeled into the controller, the controller can compensate the negative effects brought by the change of input and varying external disturbance caused by this change. Therefore, the robustness of the whole tail motion control system is enhanced. Experiments show that the robust tracking design can effectively help the robotic fish system to perform swimming gait with small relatively tracking error. Additionally, the paper illustrates the application of an analytical solution to the robust tracking problem, which is suitable for dynamic programming of the control algorithms. The controller parameters can be automatically generated by analytical equations according to the change of gait control signals. There is no need to try different parameters as what we do with

a normal PD controller. This property will be useful for future online gait generation and gait tracking where the amplitude and frequency of gait control commands keep changing during swimming. The proposed robust tracking design in this paper is applied only for the control of steady swimming gait. Future work will also focus on design of tracking controller for more versatile gait patterns.

Acknowledgements

This work is supported by the MoE AcRF RG23/06 Research Grants (Singapore), the Fundamental Research Funds for the Central Universities (China), and Zhejiang Provincial Natural Science Foundation of China under Grant No. LQ13F030001.

References

[1] J. E. Colgate and K. M. Lynch, IEEE Journal of Oceanic Engineering, vol. 29, no. 3 **(2004)**.
[2] K. H. Low and C. W. Chong, Bioinspiration & Biomimetics, vol. 5, no. 4, **(2010)**.
[3] P. Chang, "Robust Tracking and Structure from Motion with Sampling Method," Ph.D, Robotics Institute, Carnegie Mellon University, Pittsburgh, USA, **(2003)**.
[4] S. Kwon and W. K. Chung, Perturbation Compensator based Robust Tracking Control and State Estimation of Mechanical Systems, Springer, **(2004)**.
[5] J. Yu, S. Wang, and M. Tan, Robotica, vol. 23, no. 1, **(2005)**.
[6] A. Crespi, D. Lachat, A. Pasquier and A. J. Ijspeert, Autonomous Robots, vol. 25, **(2008)**, pp. 1-2.
[7] K. Seo, S. J. Chung and J. J. E. Slotine, Autonomous Robots, vol.28, no. 3, **(2010)**.
[8] H. Tan, S. Shu, and F. Lin, International Journal of Control, vol. 82, no. 3, **(2009)**.
[9] D. Dawson, Z. Quf† and J. Duffie, Robotica, vol. 11, no. 03, **(1993)**.
[10] G. V. Lauder, E. J. Anderson, J. Tangorra and P. G. A. Madden, Journal of Experimental Biology, vol. 210, no. 16, **(2007)**.
[11] C. W. Chong, Y. Zhong, C. Zhou and K. H. Low, "Can the swimming thrust of BCF biomimetic fish be enhanced?", The 2008 IEEE International Conference on Robotics and Biomimetics (ROBIO2008), Bangkok, Thailand, **(2008)**.
[12] K. H. Low, C. Zhou and Y. Zhong, Advanced Robotics, vol. 23, no. 7-8, **(2009)**.
[13] S. Saimek and P. Y. Li, International Journal of Robotics Research, vol. 23, no. 1, **(2004)**.
[14] S. Kern and P. Koumoutsakos, Journal of Experimental Biology, vol. 209, no. 24, **(2006)**.
[15] D. S. Barrett, M. S. Triantafyllou, D. K. P. Yue, M. A. Grosenbaugh and M. J. Wolfgang, Journal of Fluid Mechanics, vol. 392, **(1999)**.
[16] L. Lionel, "Underwater Robots Part II: Existing Solutions and Open Issues", Pro Literatur Verlag, Germany / ARS, Austria, **(2006)**.
[17] C. Zhou and K. H. Low, Journal of Bionic Engineering, vol. 7, **(2010)**.
[18] M. J. Lighthill, J. Fluid Mech., vol. 9, **(1960)**.
[19] H. Hu, J. Liu, I. Dukes and G. Francis, "Design of 3D swim patterns for autonomous robotic fish", IEEE/RSJ International Conference on Intelligent Robots and Systems, Beijing, China, **(2006)**.
[20] K. Singh and T. J. Pedley, Physica D: Nonlinear Phenomena, vol. 237, **(2008)**, pp. 14-17.
[21] R. C. Dorf and R. H. Bishop, "Modern Control Systems",(8th Edition), Addison Wesley Longman Inc., **(1998)**.
[22] G. F. Franklin and J. D. Powell, Feedback Control of Dynamic Systems, Prentice-Hall Inc., **(2002)**.

